

A Beating Heart Testbed for the Evaluation of Robotic Cardiovascular Interventions

Gustaaf J. Vrooijink, Hassna Irzan and Sarthak Misra

Abstract—The improved natural hemodynamics offered by mitral valve (MV) repair strategies aims to prevent heart failure and to minimize the use of long-term anticoagulant. This combined with the reduced patient trauma offered by minimally invasive surgical (MIS) interventions, requires an increase in capabilities of MIS MV repair. The use of robotic catheters have been described in MIS applications such as navigational tasks, ablation and MV repair. The majority of the robotic catheters are evaluated in testbeds capable of partially mimicking the cardiac environment (e.g., beating heart motion or relevant anatomy), while the validation of robotic catheters in a clinical scenario is associated with significant preparation time and limited availability. Therefore, continuous catheter development could be aided by an accessible and available testbed capable of reproducing beating heart motions, circulation and the relevant anatomy in MIS cardiovascular interventions. In this study, we contribute a beating heart testbed for the evaluation of robotic catheters in MIS cardiovascular interventions. Our work describes a heart model with relevant interior structures and an integrated realistic MV model, which is attached to a Stewart platform in order to reproduce the beating heart motions based on pre-operative patient data. The beating heart model is extended with an artificial aortic valve, a systemic arterial model, a venous reservoir and a pulsatile pump to mimic the systemic circulation. Experimental evaluation showed systemic circulation and beating heart motion reproduction for 70 BPM with a mean absolute distance error of 1.26 mm, while a robotic catheter in the heart model is observed by ultrasound imaging and electromagnetic position tracking. Therefore, the presented testbed is capable of evaluating MIS robotic cardiovascular interventions such as MV repair, navigation tasks and ablation.

I. INTRODUCTION

Mitral insufficiency is one of the commonly observed heart diseases in society, which requires treatment in case of hemodynamic compromise. Mitral valve (MV) repair strategies are often favored over MV replacement strategies [1]. Whereby, repair strategies aim to preserve natural hemodynamics in order to minimize the use of long-term anticoagulant [2]. MV repair is often performed by open-heart surgery via sternotomy incisions, which is associated

This research is supported by the Dutch Technology Foundation STW (iMIT-Instruments for Minimally Invasive Techniques Interactive Multi-Interventional Tools (Project: MULTI)), which is part of the Netherlands Organisation for Scientific Research (NWO) and partly funded by the Ministry of Economic Affairs, Agriculture and Innovation, and the European Research Council (ERC) under the European Unions Horizon 2020 Research and Innovation programme (Grant 638428-project ROBOTAR: Robot-Assisted Flexible Needle Steering for Targeted Delivery of Magnetic Agents). The authors are affiliated with the Surgical Robotics Laboratory, Department of Biomechanical Engineering, University of Twente, P.O. Box 217, 7500 AE Enschede, the Netherlands. S. Misra is also affiliated with the Surgical Robotics Laboratory, Department of Biomedical Engineering, University of Groningen and University Medical Center Groningen, Hanzplein 1, 9700 RB Groningen, the Netherlands.

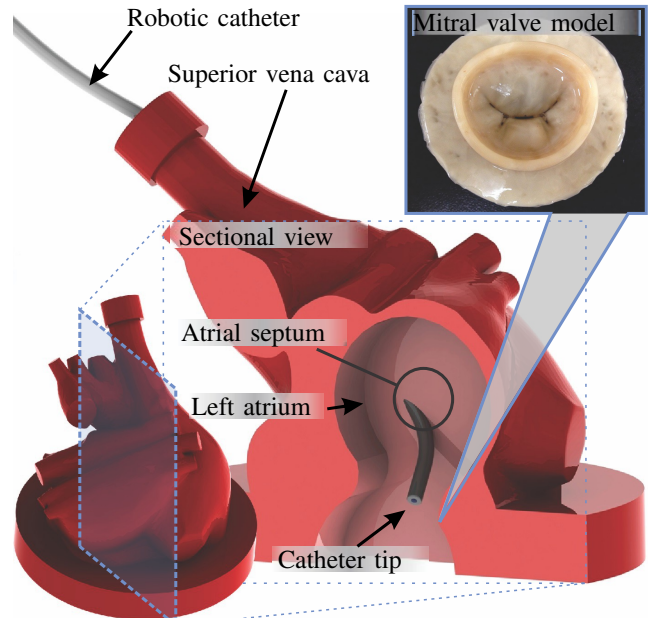


Fig. 1. A rendering of the beating heart model developed for the evaluation of robotic catheters in minimally invasive mitral valve repair surgery. The interior of the heart is modeled with an anatomically accurate superior vena cava and left and right atria, which is separated by the atrial septum. This allows a robotic catheter to be inserted in the superior vena cava into the right atrium through the atrial septum to reach a desired treatment location.

with significant patient trauma. Therefore, high-risk patients, often with comorbidities are excluded from surgery [3]. As an alternative to sternotomy incision procedures, MV repair treatment with reduced patient trauma could be provided by minimally invasive surgery (MIS) [4]. The favorable long-term outcome provided by MV repair strategies with reduced patient trauma, requires an increase in MIS capability, which can be offered by (robotic) catheter integration [5], [6].

The development of robotic catheters for cardiovascular applications have been extensively covered in literature. This includes the use of robotic catheters for navigational tasks [7]–[9]. Further, work on tele-operated systems, described the deployment of robotic catheters in applications such as endovascular surgery [10], [11]. Other studies documented the use of robotic catheters in applications such as ablation and MV repair [12]–[16]. The majority of aforementioned studies provided results obtained from experimental testbeds, which are used to partially mimic the cardiac environment (e.g., beating heart motion or relevant anatomy), while important aspects of robotic catheter evaluation in cardiovascular surgery such as fluid circulation are neglected. A small group of researchers demonstrated robotic catheter methods in *ex-* or *in-vivo* experiments. Validation

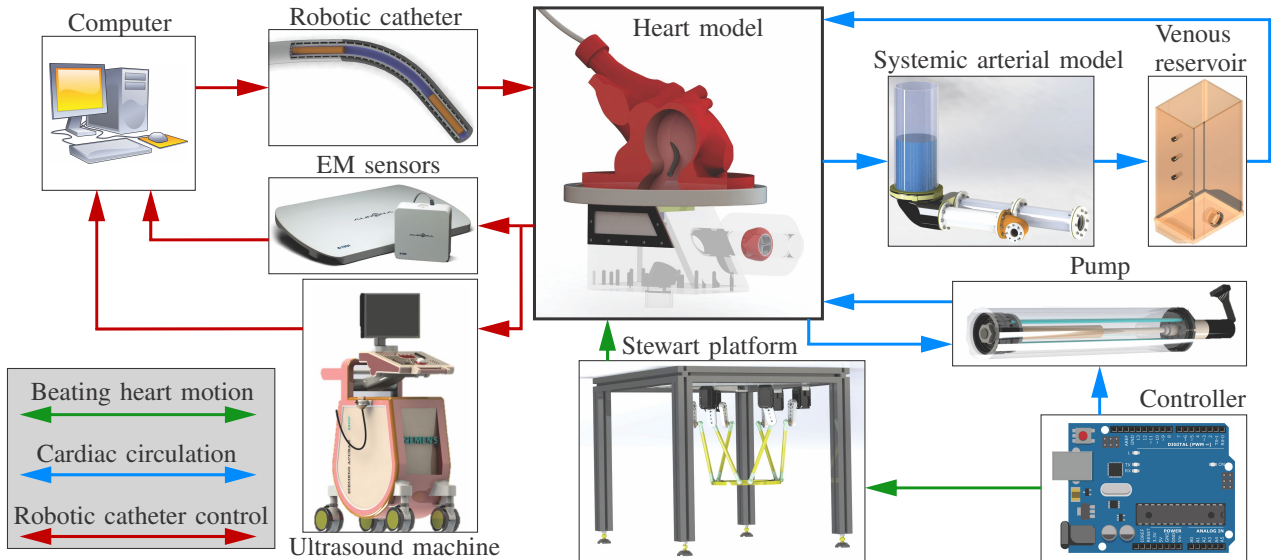


Fig. 2. An overview of the various components of the beating heart testbed associated with beating-heart MV motion reproduction (green), cardiac circulation (blue) and potential robotic catheter control (red). The heart model comprises of an interior (i.e., superior vena cava, left and right atria and atrial septum), a realistic MV, an acrylic left ventricle and an artificial aortic valve. The heart model is attached to a Stewart platform, which uses a controller to reproduce the beating heart motions based on pre-operative patient data. Systemic circulation is provided by a pulsatile pump, a systemic arterial model and a venous reservoir. A computer controlled robotic catheter could be inserted in the heart model, while feedback is provided by ultrasound images or electromagnetic (EM) position sensors.

of robotic catheters in a clinical scenario is associated with significant preparation time and limited availability. Hence, the validation of robotic catheter methods in an accessible and available testbed capable of reproducing the clinical environment could support continuous catheter development.

Various efforts in the modeling of beating heart (sub)system have been described in research. Vismara *et al.* described a pulsatile mock loop, which is used to simulate the relevant structures and fluid flow for the evaluation of aortic valves [17]. A left heart simulator was presented by Rabbah *et al.*, which is used for the study of MV mechanics and hemodynamics [18]. Mock loops that used various versions of a Windkessel model have been described by a number researchers [19]–[21]. In these studies, a Windkessel model is used to mimic resistance and compliance of the aorta and arteries of the vascular system. Further, several studies presented work capable of reproducing a realistic fluid flow and pressure during the cardiac cycle by using a pulsatile pump [22], [23]. Although, the individual components and various beating heart (sub)systems are well described in literature, these studies do not focus on the evaluation of robotically-controlled catheters in cardiovascular surgery. Further, these studies do not combine relevant aspects for robotic catheter evaluation such as beating heart motions, circulation and realistic anatomy in a single testbed.

In this study, we present a beating heart testbed developed for the evaluation of robotic catheters in cardiovascular surgery. Our work contributes a testbed, which comprises of a silicon heart model obtained from a partial cast of a bovine heart (Fig. 1). The focus of the testbed design is to provide a realistic environment for minimally invasive MV repair surgery performed by steerable and flexible robotic catheters. Hence, we model the relevant interior heart structures and integrated a realistic and functional MV. In order to reproduce

the beating heart motions at the treatment location, we attach the silicon heart model to a six degrees-of-freedom (DOF) Stewart platform. The beating heart motions at the treatment location are reproduced in three dimensional (3D) space by using pre-operative patient data. Further, we extended the beating heart model with an artificial aortic valve (AV) model and a systemic arterial model (SAM) using a Windkessel system in order to mimic the systemic circulation. A pulsatile pump is integrated in order reproduce the cardiac output by mimicking the change in ventricle volume, which enables opening and closing of the AV and MV models. Hence, the proposed beating heart testbed could provide a realistic environment for MV repair surgery. Note, that other future robotic catheter applications such as navigation, ablation and cardiac biopsy could potentially be evaluated in the presented beating heart testbed.

II. METHODS

In this section, we provide the methods used to demonstrate the beating heart testbed for the evaluation of robotic catheters in cardiovascular surgery. In section II-A, we present the experimental testbed, while in section II-B beating heart MV motion modeling is described. Subsequently, in section II-C, we describe the computer-controlled pulsatile pump. In section II-D, we provide details of systemic circulation model. Further, in the derivations presented, we use k to indicate the discrete time variable.

A. Experimental testbed

The beating heart testbed is divided in three major components, which relate to the robotic catheter control in minimally invasive MV repair surgery, the modeling of cardiac circulation and the reproduction of beating heart motions. An overview of the aforementioned components are depicted in Fig. 2, while the beating heart testbed is shown in Fig. 3.

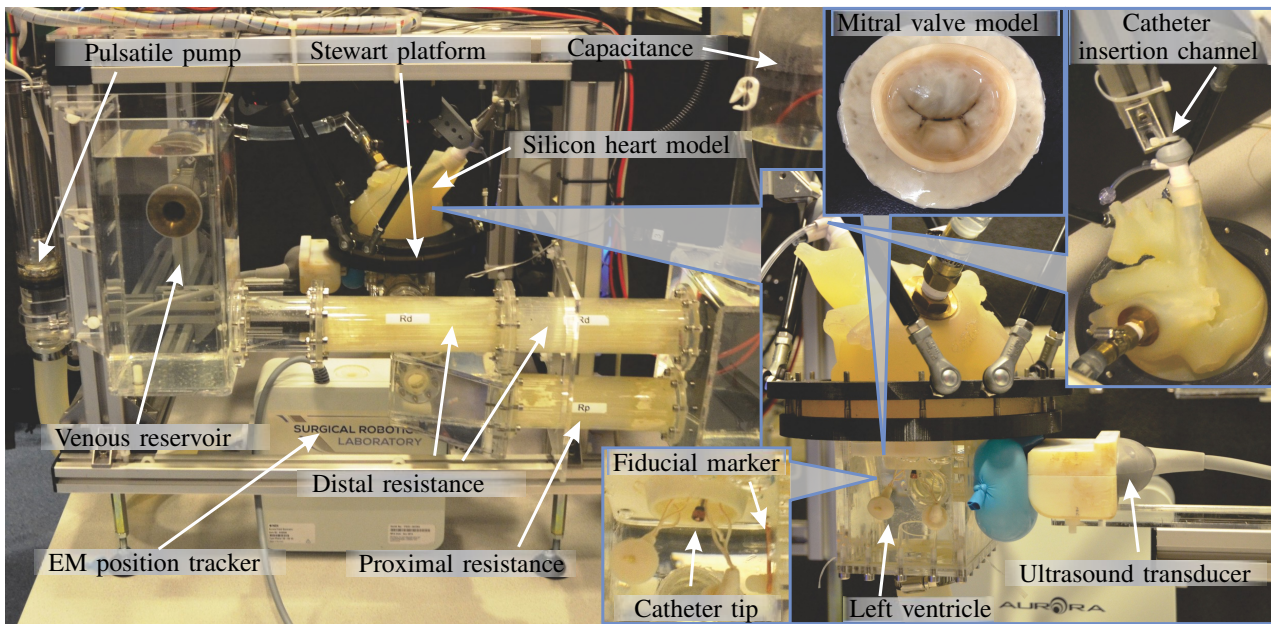


Fig. 3. An overview of the beating heart testbed for the evaluation of robotic cardiovascular interventions. The beating heart testbed comprises of a silicon heart model with an embedded mitral valve model (top inset) and an acrylic left ventricle model. In order to mimic systemic fluid flow, the silicon heart model is extended by a pulsatile pump and a systemic arterial model with a proximal resistance, a distal resistance, a capacitance and a venous reservoir. The heart model is attached to a Stewart platform in order to mimic the beating heart motions at the treatment location. Further, a robotic catheter insertion channel (top right inset) provides access to the mitral valve via the superior vena cava, while electromagnetic (EM) position tracking is provided.

In this study, robotic catheter control in minimally invasive MV repair is considered. Hence, we use silicon heart model obtained from a partial cast of a bovine heart. The interior of the silicon heart is modeled with an anatomical correct superior vena cava and left and right atria, which is separated by a atrial septum. Further, we integrated a functional and realistic MV model with an implemented anterior and posterior middle prolapse (LifeLike BioTissue Inc., London, Canada) in the silicon heart model. This allows for a robotic catheter to be inserted in the superior vena cava into the right atrium through the atrial septum to reach a desired treatment location such as the MV. By considering a water-filled bellows, the MV including the robotic catheter could be observed by ultrasound imaging as depicted in Fig. 2. The water-filled bellows enables the transmission of ultrasound waves from a stationary transducer to the moving heart model during the reproduction of beating heart motions. Note, that a stationary transducer introduces simplifications compared to clinical practice. A fiducial marker is integrated in the testbed as shown in Fig. 2, which can be used to evaluate the reproduced beating heart motions of the heart model in ultrasound images. The observed beating heart motion in ultrasound images could be considered as a reference signal for closed-loop control of a robotic catheter. Complementary or as an alternative to ultrasound imaging, electromagnetic (EM) tracking sensors embedded in the catheter could be used for instrument feedback. By minimizing the use of interfering materials such as ferromagnetic and electrically conductive materials in and near the heart model, EM positional tracking of the robotic catheter is not impeded [24].

The functional opening and closing of the integrated MV model is provided by systemic circulation. Hence, we extend

the heart model with an acrylic left ventricle, an artificial AV and a SAM. The SAM comprises of a proximal resistor, a distal resistor and a capacitance element, which is used to mimic resistance and expansion of the vascular system, respectively. A venous reservoir is included in the systemic circulation to serve as a buffer between the distal resistor and left atrium of the heart model. Note, that by neglecting the pulmonary circulation circuit, we introduce simplifications compared to clinical practice. Further, we attach an automated pump to the left ventricle of the heart model, which is used to reproduce the cardiac output by mimicking the change in ventricle volume. The pump is controlled by an Arduino Due (Arduino, Somerville, USA) and comprises of a piston positioned by a GP22S ball screw spindle drive with a pitch of 2 mm per rotation, which is attached to a ECMax22 motor (Maxon Motor, Sachseln, Switzerland).

In order to reproduce the beating heart motions at the treatment location (i.e., MV) in 3D space, we attach the heart model to a six DOF Stewart platform [25]. The Stewart platform is actuated by six MX-64AR servo motors (ROBOTIS Co., Ltd., Seoul, South Korea) and controlled by an Arduino Due. The reproduced beating heart motions are obtained from pre-operative patient data by using 3D magnetic resonance images of a MV. Further, we consider the heart-rate variability in the reproduced beating heart motions.

B. Beating heart mitral valve motion modeling

In this section, we describe the model used to reproduce the beating heart MV motions in 3D space, which is obtained by pre-operative patient data using 3D magnetic-resonance (MR) images. The MR volume (seven slices of 256 by 256 pixels) data are obtained with a rate of 30 volumes-

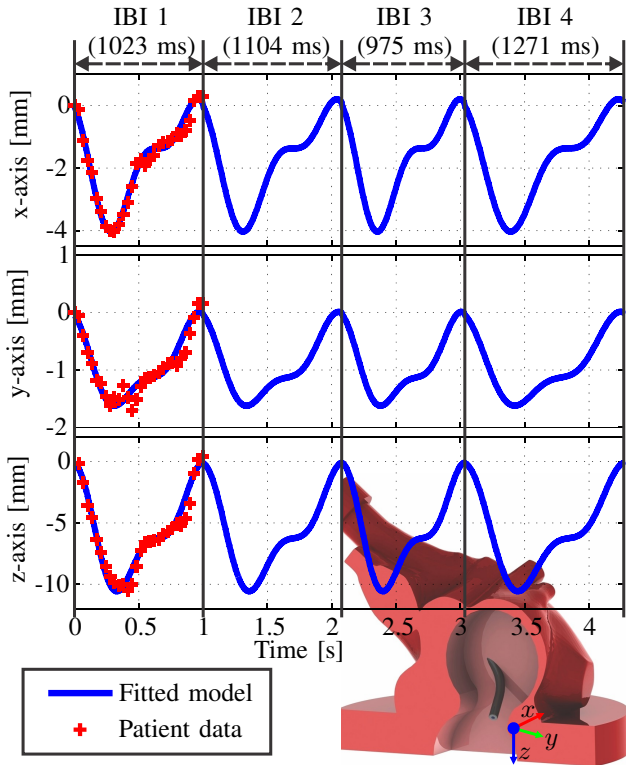


Fig. 4. The beating heart mitral valve motions obtained from pre-operative patient data (red cross) and the corresponding fitted model (blue line). The fitted model is described by a two-term Fourier series, which is used to reproduce the periodic motion of the beating heart mitral valve in 3D space. Further, heart rate variability modeling is introduced to simulate the beat-to-beat variation, which is indicated by inter-beat intervals (IBI) 1 to 4.

per-second by a 1.5 Tesla imaging scanner using a transesophageal echocardiogram (TEE) system (Philips Healthcare, Amsterdam). Manual segmentation is used to obtain the motion path of the MV over the cardiac cycle. More details are provided in previous work, where the beating heart MV motions are reproduction in two-dimensional (2D) space [25]. The 3D periodic beating heart MV motion is obtained from manual segmentation, which can be described by a two-term Fourier series according to

$$r_* = a_{0*} + a_{1*} c\left(\frac{k}{S_r} \omega\right) + b_{1*} s\left(\frac{k}{S_r} \omega\right) + a_{2*} c\left(2\frac{k}{S_r} \omega\right) + b_{2*} s\left(2\frac{k}{S_r} \omega\right), \quad (1)$$

where $*$ denotes the associated x -, y - and z -axis, k the discrete time variable, S_r is the sample rate and ω denotes the frequency of the periodic motion. However, by considering a constant frequency (ω) of the periodic beating heart MV motions, the heart rate variability (HRV) is not taken into account. HRV is generated by heart and brain interactions, which is controlled by the autonomic nervous system. HRV is described by the inter-beat interval (IBI), which is the time period between successive heart beats (Fig. 4). The HRV frequency is considered to be < 0.4 Hz. Further, the standard deviation (SDNN) of the beat-to-beat or NN intervals for patients with SDNN values below 50 milliseconds (ms) are classified as unhealthy, 50 to 100 ms have compromised health, and above 100 ms are considered healthy [26]. HRV often poses a challenge for the (predictive) control of robotic catheters. Hence, we use a uniform distribution

model ($\mathcal{U}(t_1, t_2)$) to describe the HRV according to

$$\omega = \omega_{h_r} + 2\pi\mathcal{U}(t_1, t_2), \quad (2)$$

where the HRV interval is given by $t_1 = -200$ ms and $t_2 = 200$ ms, while the standard deviation is given by $\frac{1}{2*\sqrt{3}} * (t_2 - t_1) = 115$ ms. Further, the frequency (ω_{h_r}) can be computed according to $\omega_{h_r} = \frac{2\pi}{60} h_r$, where h_r is the heart rate in beats-per-minute (BPM), which is used in (2) to evaluate the variable frequency (ω). By considering the variable frequency (ω) and the two-term Fourier series in (1), we can reproduce beating heart motions with HRV.

C. Cardiac pump

In order to provide a fluid flow in the heart model, we attach an automated pulsatile pump to the left ventricle of the heart model. The pulsatile pump is used to mimic the left ventricle volume as depicted in Fig. 5. The cardiac cycle comprises of systole and diastole phases, where the stroke volume (l_{sv}) can be evaluated by the end-diastolic volume subtracted by the end-systolic volume. In this study we use a stroke volume of 70 mL, which is observed in clinical practice. By considering the stroke volume (l_{sv}), the total pump displacement l_d is given by

$$l_d = \frac{l_{sv}}{\pi r_p^2}, \quad (3)$$

where r_p is the piston radius. Note, that the ventricle volume changes during the systole (i.e., isovolumic contraction, ejection) and diastole (i.e., isovolumic relaxation, rapid filling, diastasis and atrial systole) phases as depicted in Fig. 5 [27]. Hence, by considering the aforementioned phases and the left ventricle volume as depicted in Fig. 5, we used a Fourier series of six terms in order to mimic the ventricle volume ($V(k)$) during the cardiac cycle according to

$$\begin{aligned} V(k) = & a_{0_p} + a_{1_p} c\left(\frac{k}{S_r} \omega\right) + b_{1_p} s\left(\frac{k}{S_r} \omega\right) + \\ & a_{2_p} c\left(2\frac{k}{S_r} \omega\right) + b_{2_p} s\left(2\frac{k}{S_r} \omega\right) + a_{3_p} c\left(3\frac{k}{S_r} \omega\right) + b_{3_p} s\left(3\frac{k}{S_r} \omega\right) + \\ & a_{4_p} c\left(4\frac{k}{S_r} \omega\right) + b_{4_p} s\left(4\frac{k}{S_r} \omega\right) + a_{5_p} c\left(5\frac{k}{S_r} \omega\right) + b_{5_p} s\left(5\frac{k}{S_r} \omega\right) + \\ & a_{6_p} c\left(6\frac{k}{S_r} \omega\right) + b_{6_p} s\left(6\frac{k}{S_r} \omega\right), \quad (4) \end{aligned}$$

where $s(*) = \sin(*)$ and $c(*) = \cos(*)$, the Fourier coefficients are given by $a_{0_p} = 35.03$, $a_{1_p} = 24.34$, $b_{1_p} = -21.77$, $a_{2_p} = 6.40$, $b_{2_p} = 4.57$, $a_{3_p} = 4.36$, $b_{3_p} = -0.91$, $a_{4_p} = -0.03$, $b_{4_p} = 1.61$, $a_{5_p} = -0.19$, $b_{5_p} = 1.06$, $a_{6_p} = -0.24$ and $b_{6_p} = 1.15$, while the corresponding goodness of fit is

TABLE I

TABLE OF FOURIER COEFFICIENTS USED TO MODEL THE PERIODIC MITRAL VALVE MOTIONS IN (1), WHICH ARE OBTAINED FROM PRE-OPERATIVE PATIENT DATA BY USING 3D MAGNETIC-RESONANCE IMAGING. SUBSCRIPT $*$ INDICATES THE ASSOCIATED x -, y AND z -AXIS, WHILE THE SQUARE OF THE CORRELATION IS DENOTED (R^2).

axis	a_{0*}	a_{1*}	b_{1*}	a_{2*}	b_{2*}	R^2
x	-1.735	0.888	-1.413	0.804	-0.006	0.98
y	-0.906	0.584	-0.363	0.273	-0.050	0.93
z	5.626	-3.648	2.019	-1.834	-0.504	0.97

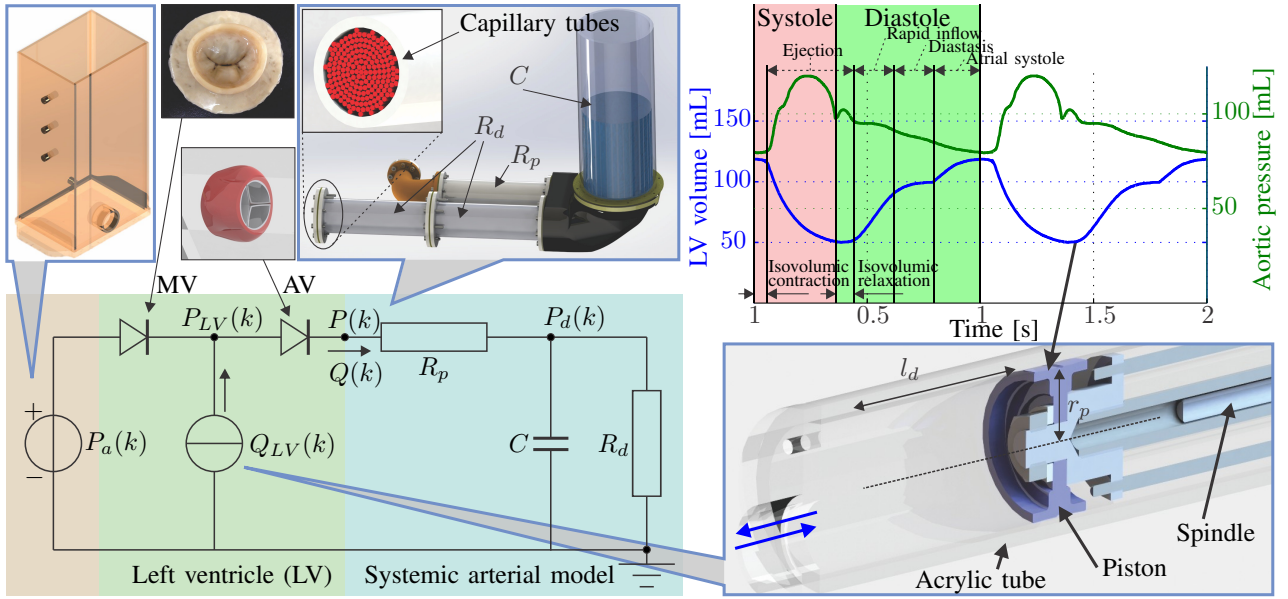


Fig. 5. An overview of systemic circulation modeling with integrated mitral valve (MV) and aortic valve (AV). A three-element Windkessel model with capacitance (C), proximal resistance (R_p) and distal resistance (R_d) is used to mimic the left ventricle (LV) pressure ($P_{LV}(k)$), the aortic pressure ($P(k)$) and distal systemic pressure ($P_d(k)$), while a fixed filling pressure ($P_a(k)$) is provided by a venous reservoir (Top left inset). A pulsatile pump with piston radius (r_p) and displacement (l_d) is attached to the LV of the heart model. The pump provides a LV fluid flow ($Q_{LV}(k)$) and aortic fluid flow ($Q(k)$), which is described by the time derivative of the LV volume. The top right inset provides the LV volume and aortic pressure as described in literature [27].

given by the square of the correlation ($R^2 = 0.99$). Further, the HRV model described (2) can be used in the left ventricle volume model provided in (4), which is used in systemic circulation reproduction.

D. Systemic circulation modeling

In order to provide realistic opening and closing of the MV and AV, we mimic the impedance of the systemic arterial system by using a systemic arterial model (SAM). A three-element Windkessel model can be used to describe the pressure and flow relation at the entrance of the systemic arterial system. The SAM as depicted in Fig. 5 comprises of a capacitance (C) and proximal and distal resistors, (R_p) and (R_d), respectively. By considering a distal location in the SAM, the relation between the aortic fluid flow ($Q(k)$) and the aortic pressure ($P(k)$) and pressure ($P_d(k)$) at a distal location is given by

$$P(k) - P_d(k) = R_p Q(k). \quad (5)$$

Further, the left ventricle volume ($V(k)$) described in (4) can be used to find an expression for the fluid flow ($Q(k)$) through the AV entering the SAM according to

$$Q(k) = \begin{cases} -\Delta V(k) & \text{for } k \in [t_n, t_n + t_s] \\ 0 & \text{for } k \in [t_n + t_s, t_n + t_s + t_d] \end{cases}, \quad (6)$$

where t_n indicates the start time of the cardiac cycle and t_s and t_d the systole and diastole times, respectively. The relation between fluid flow ($Q(k)$) described in (6) and the distal pressure ($P_d(k)$) is described by a two-element Windkessel model as follows:

$$Q(k) = C \Delta P_d(k) + \frac{1}{R_d} P_d(k), \quad (7)$$

where $\Delta P_d(k)$ is the discrete time derivative of the distal pressure ($P_d(k)$). The two-element Windkessel model can be extended to a three-element Windkessel model by rearranging the distal pressure ($P_d(k)$) in (5), which can be substituted into (7) according to

$$C R_p \Delta Q(k) + \frac{R_d + R_p}{R_d} Q(k) = C \Delta P(k) + \frac{1}{R_d} P(k), \quad (8)$$

where $\Delta Q(k)$ is the discrete time derivative of the fluid flow ($Q(k)$) described in (6), thus known. By considering the differential equation in (8), the modeled fluid flow in (6) and the aortic pressure described by literature as shown in Fig. (5), we can estimate for the proximal resistance ($R_p = 0.075$ mmHg·s/mL), distal resistance ($R_p = 1.25$ mmHg·s/mL) and capacitance ($C = 1.9$ mL/mmHg).

The proximal and distal resistances (R_*) can be obtained by N_* parallel capillary tubes with length (l_*) and radius (r_*) using the Hagen-Poiseuille equation according to

$$R_* = \frac{P_*(k)}{Q_*(k)} = \frac{8\mu l_*}{\pi N_* r_*^4} \Rightarrow N_* = \frac{8\mu l_*}{\pi R_* r_*^4}, \quad (9)$$

where $*$ = p and $*$ = d are associated with the proximal and distal resistances, respectively. Further, $P_*(k)$ describes the pressure loss, $Q_*(k)$ is the fluid flow and μ represents the dynamic viscosity of blood (0.029 g/cm/s). By considering the density of blood ($\rho = 1060.0$ kg/m³) and the Reynolds number for laminar flow in a capillary tube according to

$$Re = \frac{2\rho}{\pi\mu N_* r_*} Q(k) < 2300, \quad (10)$$

we evaluate the capillary tube lengths ($l_p = 150$ and $l_d = 300$ mm), the radii ($r_p = 0.0775$ and $r_d = 0.04$ mm) and the total parallel tubes ($N_p = 307$ and $N_d = 519$). Hence, we complete the systemic circulation modeling.

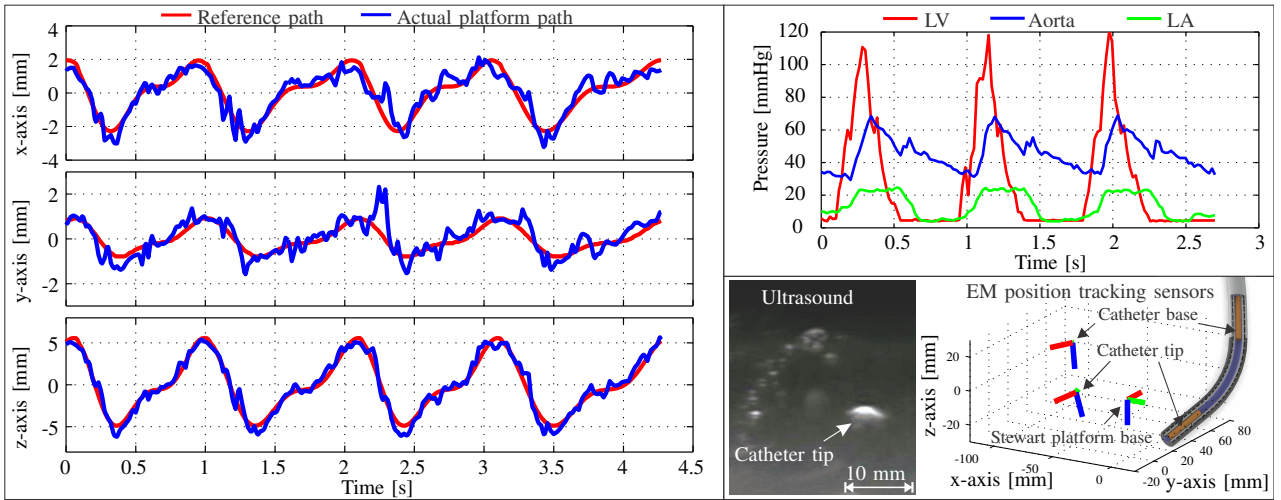


Fig. 6. Representative experimental results of beating heart motion reproduction in three dimensions (left) and systemic circulation (top-right) for a heart rate of 60 BPM. The motion reference path is depicted red, while the actual platform path is shown in blue, which is measured by an electromagnetic (EM) sensor attached to the moving Stewart platform. The systemic circulation is provided by a pulsatile pump, while the pressure in the left ventricle (LV) (red), aorta (blue) and left atrium (LA) (blue) are measured. Further, the bottom-right inset demonstrates ultrasound observations and an EM position measurement of a robotic catheter inserted in the beating heart model.

III. EXPERIMENTS

In this section, the experimental plan used to evaluate the beating heart testbed is described and the corresponding results are presented.

A. Experimental plan

The experimental plan comprises of three parts. First we evaluate the reproduction of beating heart MV motions including HRV in 3D space based on pre-operative patient data described in section II-B. The reproduced motion is evaluated by using a five DOF EM sensor (Northern Digital Inc., Ontario, Canada), which is attached to the moving Stewart platform. Subsequently, we evaluate the proposed systemic circulation model described in section II-D by using MPX5050GP pressure sensors (NXP Semiconductors, Eindhoven, the Netherlands). Finally, we demonstrate ultrasound and EM observation of a stationary robotic catheter inserted in the MV of the beating heart model. The stationary robotic catheter is observed by a Siemens Acuson S2000™ ultrasound system with a Siemens 18L6 transducer (Siemens AG, Erlangen, Germany) and by two embedded EM sensors (Northern Digital Inc., Ontario, Canada).

B. Results

The experimental results of the beating heart motion reproduction are provided in Table II, while a representative experiment is depicted in the left plot of Fig. 6. Further, the experimental results of system circulation reproduction using a pulsatile pump, a SAM and a venous reservoir are depicted in the top-right inset (Fig. 6), while the observations of a stationary robotic catheter in ultrasound and EM position tracking are provided in the bottom-right inset (Fig. 6).

Experiments in reproducing the beating heart motion show a mean absolute distance error (ϵ) of approximately 0.8 mm for heart rates of 20 to 50 BPM, while a deterioration for heart rates of 60 and 70 BPM of 1.07 and 1.26 mm are observed, respectively. Note, that changing heart rates could

be considered during catheter evaluation. The deterioration for higher heart rates (i.e., 60 and 70 BPM) could potentially be attributed to the tubes between the fixed elements of the SAM and the beating heart model attached to the moving Stewart platform.

Further, systemic circulation experiments showed that the change in LV volume provided by the pulsatile pump results in a maximum LV pressure of approximately 120 mmHg, while the observed maximum aortic pressure and the corresponding decay is approximately 70 and 35 mmHg, respectively. Note, that the reduced aortic pressure in experiments compared to clinical practice (top-right inset, Fig. 5) did not limit AV and MV opening and closing, which is considered in catheter evaluation. The difference between LV and aortic pressure indicates a resistance introduced by the artificial AV, which is similar to AV stenosis. The pressure in the left atrium (LA) during the systole increases to approximately 25 mmHg. This could be attributed to the MV with implemented prolapse, which causes MV regurgitation.

Further, observations of a stationary robotic catheter inserted in the beating heart model are provided in Fig. 6. Observations showed that the catheter is visible in ultrasound images and could be tracked by two embedded EM position sensors as provided in the bottom-right inset (Fig. 6).

TABLE II

THE RESULTS OF THE BEATING HEART TESTBED MOTION REPRODUCTION EXPERIMENTS FOR HEART RATES OF 20 TO 70 BPM. THE MEAN ABSOLUTE DISTANCE ERROR (ϵ) AND THE MEAN ABSOLUTE POSITION ERRORS (ϵ_x , ϵ_y AND ϵ_z) ARE PROVIDED WITH THE STANDARD DEVIATION OF THE ABSOLUTE ERROR.

BPM	ϵ_x [mm]	ϵ_y [mm]	ϵ_z [mm]	ϵ [mm]
20	0.17	0.31	0.63	0.79 ± 0.53
30	0.26	0.38	0.57	0.80 ± 0.52
40	0.24	0.33	0.47	0.70 ± 0.40
50	0.24	0.36	0.60	0.81 ± 0.57
60	0.33	0.49	0.78	1.07 ± 0.70
70	0.34	0.52	0.98	1.26 ± 0.95

IV. CONCLUSIONS AND FUTURE WORK

In this study, we described an experimental testbed for the evaluation of robotic cardiovascular interventions. We presented a beating heart model with a realistic interior, a realistic MV and an artificial AV. The heart model is attached to a Stewart platform in order to reproduce the beating heart motions based on pre-operative patient data. Further, systemic circulation is obtained by a pulsatile pump, a SAM and a venous reservoir. This provides a realistic cardiac environment for MIS MV repair surgery. In experiments, we demonstrated beating heart motion reproduction with an error of 1.26 mm for heart rates of 70 BPM, while the observed maximum LV and aortic pressures are approximately 120 and 70 mmHg, respectively. Further, we provided observations of a stationary catheter in the heart model by using ultrasound images and EM position tracking, which can be used in closed-loop control of robotic instruments.

In future work, we intend to perform robotic catheter studies in the beating heart testbed. Further, we aim to expand the testbed by considering various aortic and mitral valves in order to mimic different cardiac diseases. By considering different realistic valvular models, cardiac decreases such as insufficiency and stenosis could be mimicked, while a robotic catheter could demonstrate effective treatment. Our proposed experimental testbed demonstrates cardiac motion and circulation reproduction with integrated valve models. Therefore, the presented experimental testbed could provide a platform for the evaluation of future robotic catheter applications such as MV repair, navigational tasks and ablation.

REFERENCES

- [1] A. B. Goldstone, J. E. Cohen, J. L. Howard, B. B. Edwards, A. L. Acker, W. Hiesinger, J. W. M. Jr., P. Atluri, and J. Y. Woo, "A repair-all strategy for degenerative mitral valve disease safely minimizes unnecessary replacement," *The Annals of Thoracic Surgery*, vol. 99, no. 6, pp. 1983–1991, 2014.
- [2] S. F. Bolling, S. Li, S. M. O'Brien, J. M. Brennan, R. L. Prager, and J. S. Gammie, "Predictors of mitral valve repair: Clinical and surgeon factors," *The Annals of Thoracic Surgery*, vol. 90, no. 6, pp. 1904–1912, 2010.
- [3] O. De Backer, N. Piazza, S. Banai, G. Lutter, F. Maisano, H. C. Herrmann, O. W. Franzen, and L. Søndergaard, "Percutaneous transcatheter mitral valve replacement," *Circulation: Cardiovascular Interventions*, vol. 7, no. 3, pp. 400–409, 2014.
- [4] J. Y. Woo, E. Rodriguez, P. Atluri, and W. R. Chitwood, Jr, "Minimally invasive, robotic, and off-pump mitral valve surgery," *Seminars in Thoracic and Cardiovascular Surgery*, vol. 18, no. 2, pp. 139–147, 2006.
- [5] W. R. Chitwood Jr, "Robotic mitral valve surgery: overview, methodology, results, and perspective," *Annals of Cardiothoracic Surgery*, vol. 5, no. 6, pp. 544–555, 2016.
- [6] D. A. Murphy, E. Moss, J. Binongo, J. S. Miller, S. K. Macheers, E. L. Sarin, A. M. Herzog, V. H. Thourani, R. A. Guyton, and M. E. Halkos, "The expanding role of endoscopic robotics in mitral valve surgery: 1,257 consecutive procedures," *The Annals of Thoracic Surgery*, vol. 100, no. 5, pp. 1675–1682, 2015.
- [7] Y. Ganji, F. Janabi-Sharifi, and A. N. Cheema, "Robot-assisted catheter manipulation for intracardiac navigation," *International Journal of Computer Assisted Radiology and Surgery*, vol. 4, no. 4, pp. 307–315, 2009.
- [8] J. Jayender, R. V. Patel, and S. Nikumb, "Robot-assisted active catheter insertion: Algorithms and experiments," *The International Journal of Robotics Research*, vol. 28, no. 9, pp. 1101–1117, 2009.
- [9] N. Xiao, P. Guo, and S. Guo, "Push force feedback for a kind of robotic catheter navigation system," in *Proceedings of the IEEE International Conference on Information and Automation*, pp. 32–37, Lijiang, China, August 2015.
- [10] X. Yin, S. Guo, H. Hirata, and H. Ishihara, "Design and experimental evaluation of a teleoperated haptic robot-assisted catheter operating system," *Journal of Intelligent Material Systems and Structures*, vol. 27, no. 1, pp. 3–16, 2016.
- [11] B. Rosa, A. Devreker, H. D. Praetere, C. Gruijthuijsen, S. Portoles-Diez, A. Gijbels, D. Reynaerts, P. Herijgers, J. V. Sloten, and E. V. Poorten, "Intuitive teleoperation of active catheters for endovascular surgery," in *Proceedings of the IEEE International Conference on Intelligent Robots and Systems (IROS)*, pp. 2617–2624, Hamburg, Germany, September 2017.
- [12] J. Gangloff, R. Ginhoux, M. de Mathelin, L. Soler, and J. Marescaux, "Model predictive control for compensation of cyclic organ motions in teleoperated laparoscopic surgery," *IEEE Transactions on Control Systems Technology*, vol. 14, no. 2, pp. 235–246, 2006.
- [13] A. H. Gosline, N. V. Vasilyev, E. J. Butler, C. Folk, A. Cohen, R. Chen, N. Lang, P. J. del Nido, and P. E. Dupont, "Percutaneous intracardiac beating-heart surgery using metal ments tissue approximation tools," *The International Journal of Robotics Research*, vol. 31, no. 9, pp. 1081–1093, 2012.
- [14] S. B. Kesner and R. D. Howe, "Robotic catheter cardiac ablation combining ultrasound guidance and force control," *The International Journal of Robotics Research*, vol. 33, no. 4, pp. 631–644, 2014.
- [15] G. J. Vrooijink, A. Denasi, J. G. Grandjean, and S. Misra, "Model predictive control of a robotically actuated delivery sheath for beating heart compensation," *The International Journal of Robotics Research*, vol. 36, no. 2, pp. 193–209, 2017.
- [16] P. M. Loschak, A. Değirmenci, and R. D. Howe, "Predictive filtering in motion compensation with steerable cardiac catheters," in *Proceedings of the IEEE International Conference on Robotics and Automation (ICRA)*, pp. 4830–4836, Singapore, Singapore, May 2017.
- [17] R. Vismara, G. B. Fiore, A. Mangini, M. Contino, M. Lemma, A. Redaelli, and C. Antona, "A novel approach to the in vitro hydrodynamic study of the aortic valve: Mock loop development and test," *American Society for Artificial Internal Organs*, vol. 56, no. 4, pp. 279–284, 2010.
- [18] J.-P. Rabbah, N. Saikrishnan, and A. P. Yoganathan, "A novel left heart simulator for the multi-modality characterization of native mitral valve geometry and fluid mechanics," *Annals of biomedical engineering*, vol. 41, no. 2, pp. 305–315, 2013.
- [19] N. Westerhof, J.-W. Lankhaar, and B. E. Westerhof, "The arterial windkessel," *Medical & Biological Engineering & Computing*, vol. 47, no. 2, pp. 131–141, 2009.
- [20] E. O. Kung and C. A. Taylor, "Development of a physical windkessel module to re-create in-vivo vascular flow impedance for in-vitro experiments," *Cardiovascular engineering and technology*, vol. 2, no. 1, pp. 2–14, 2011.
- [21] K. Her, J. Y. Kim, K. M. Lim, and S. W. Choi, "Windkessel model of hemodynamic state supported by a pulsatile ventricular assist device in premature ventricle contraction," *BioMedical Engineering OnLine*, vol. 17, no. 1, pp. 1–13, 2018.
- [22] R. A. Chaudhury, V. Atlasman, G. Pathangey, N. Pracht, R. J. Adrian, and D. H. Frakes, "A high performance pulsatile pump for aortic flow experiments in 3-dimensional models," *Cardiovascular Engineering and Technology*, vol. 7, no. 2, pp. 148–158, 2016.
- [23] R. R. Mechoor, T. Schmidt, and E. Kung, "A real-time programmable pulsatile flow pump for in vitro cardiovascular experimentation," *Journal of Biomechanical Engineering*, vol. 138, no. 11, pp. 1–5, 2016.
- [24] A. M. Franz, T. Haidegger, W. Birkfellner, K. Cleary, T. M. Peters, and L. Maier-Hein, "Electromagnetic tracking in medicine - a review of technology, validation, and applications," *IEEE Transactions on Medical Imaging*, vol. 33, no. 8, pp. 1702–1725, 2014.
- [25] G. J. Vrooijink, M. P. Jansen, M. L. Tolhuisen, J. G. Grandjean, and S. Misra, "Ultrasound-guided stabilization of a robotically-actuated delivery sheath (rads) for beating heart mitral valve motions," in *Proceedings of the IEEE International Conference on Biomedical Robotics and Biomechanics*, pp. 73–79, Singapore, June 2016.
- [26] F. Shaffer and J. P. Ginsberg, "An overview of heart rate variability metrics and norms," *Frontiers in Public Health*, vol. 5, no. 258, 2017.
- [27] J. R. Mitchell and J. Wang, "Expanding application of the wiggers diagram to teach cardiovascular physiology," *Advances in Physiology Education*, vol. 38, no. 2, pp. 170–175, 2014.